Measurement of the Beam Size at SR Center of Ritsumeikan University by the SR Interferometer

Yasukazu YAMAMOTO, Ichiro SAKAI*, Toshiyuki MITSUHASHI**,
Daizo AMANO*** and Hiroshi IWASAKI
SR center, Ritsumeikan University, Kusatsu, Shiga 525-8577, Japan
*Faculty of Science and Engineering, Ritsumeikan University, Kusatsu, Shiga 525-8577, Japan
**High Energy Accelerator Research Organization, Oho, Tsukuba, Ibaraki 305-0801, Japan
***Research & Development Center, Sumitomo Heavy Industries, Tanashi, Tokyo 188-8585, Japan

Abstract

The beam size in the compact superconducting storage ring at SR center of Ritsumeikan University was measured using the SR interferometer (interferometer for synchrotron radiation) developed by one of the present authors. The spatial coherence of the radiation beam in visible range was measured at the region of spatial frequency from 25.0 to 140.4 mm^{-1}. Analysis of the data has yielded the beam size to be 10.5μm in the vertical direction. The beam size was also measured for the large beam controlled by RF kicker, and the lifetime was measured at the same time. The lifetimes observed for small beam size agreed with the theoretical lifetime (Touschek lifetime).

1. Introduction

The beam size in the electron storage ring is an important parameter for the use of the radiation emitted. In many synchrotron radiation facilities, the focusing-lens imaging method were employed to observed the beam size. The resolution of this method is limited by diffraction phenomena, the size smaller than 50μm can not accurately be measured. Recently one of the present author (T.M) developed a new method, in which the van Cittert-Zernike's theorem[1] was applied to lead to the determination of the beam size[2]. It is applicable to the measurement of the beam size of the order of 1μm.

The beam size of AURORA at SR center of Ritsumeikan University was estimated of the order of 10μm in the vertical direction by means of the lifetime of the stored electron beam[3]. We have applied the SR-interferometer to the measurement of the vertical beam size.

2. Spatial Coherence and Beam Profile

According to van Cittert-Zernike's theorem, the complex degree of spatial coherence $\gamma(\upsilon)$ is given as a Fourier transform of the object profile $f(y_0)$ as follows;

$$\gamma(\upsilon) = \int f(y_0)\exp\{-i\upsilon y_0\}dy_0, \qquad (1)$$

where υ is the spatial frequency, y_0 is the position on the source plane. $\gamma(\upsilon)$ can be obtained from the intensity profile $I(y_1)$ of an interferogram formed using the interferometer through the relation

$$I(y_1) = I_0\left[1+\gamma(\upsilon)\cos\left(\frac{2\pi D}{\lambda R_1}y_1\right)\right]\left[\mathrm{sinc}\left(\frac{2\pi a}{\lambda R_1}y_1\right)\right]^2, \qquad (2)$$

the y_1 being position on the observation plane, D the double slit separation, λ the wave length of light, R_1 the distance between the secondary principal point of the lens and the interferogram, a the half of the slit height, R_0 the distance between the object beam and the double slit.

3. SR Interferometer

The SR interferometer is basically of the wavefront-division two beam type using polarized quasimonochromatic rays. The SR interferometer was set up at BL-9 of AURORA at a distance of 3750mm from the source point. The opening angle in vertical plane was fixed to 11mrad by the slit of the radiation damper. A thick beryllium mirror is set to reflect the primary beam to extract the visible component. An aperture of 1x1mm was used in the double slits assembly. A diffraction limited doublet-lens with the focal length f=600 mm was used as an objective lens of the interferometer. The slit separation D is variable from 6.7mm to 37.7mm, corresponding range of the

spatial frequency υ being from 25.0mm^{-1} to 140.4mm^{-1}. The band-pass filter centered at 450nm and the polarization filter are inserted in the beam path. A schematic drawing of the SR interferometer is shown in Fig. 1.

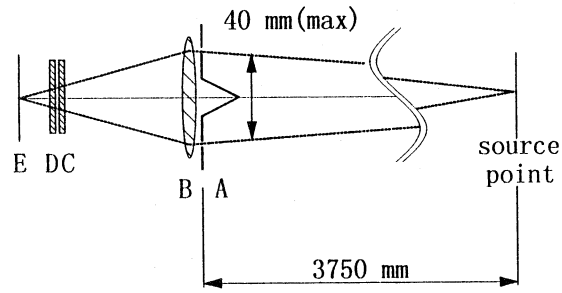

Fig. 1 Structure of the SR interferometer. A: double-slit; B: diffraction limited doublet-lens; C: polarization filter; D: band-pass filter (λ=450nm, $\Delta\lambda$=10nm); E: interferogram.

4. Result of Degree of Spatial Coherence and Vertical Beam Profile

Figure 2 shows an measured interferogram $I(y_1)$ at υ=28.7mm^{-1} (D=7.7mm). The spatial coherence $\gamma(\upsilon)$ is evaluated from the visibility of the interferogram. Figure 3 shows the spatial coherence $\gamma(\upsilon)$ plotted as a function of spatial frequency. Assuming the Gaussian profile, the beam size(σ_y) can be calculated from the spatial coherence $\gamma(\upsilon)$ by using the formula given by

$$\gamma(\upsilon) = \exp\left(-\frac{\sigma_y^2}{2}\upsilon^2\right). \qquad (3)$$

Least squares fitting has yielded σ_y to be 10.5μm. Almost the same value was obtained from the measurements using the radiation of another wavelength, 520nm.

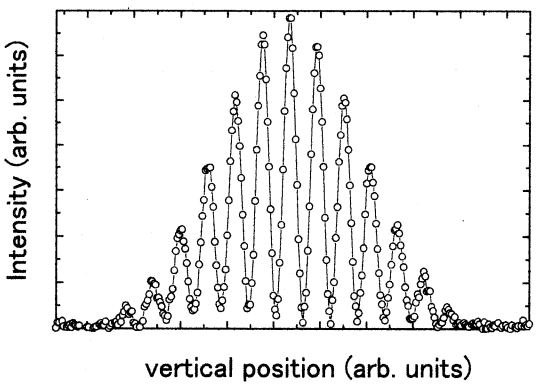

Fig. 2 The measured interferogram at υ=28.7mm^{-1} (D=7.7mm), λ=450nm.

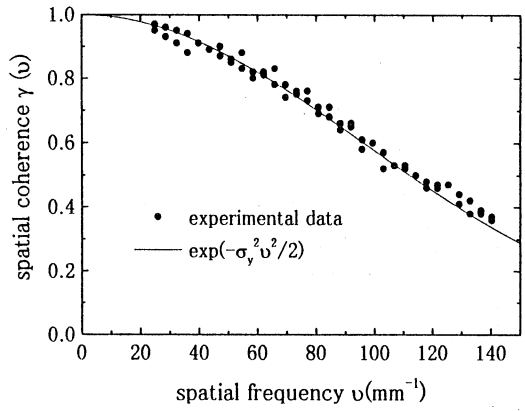

Fig. 3 Spatial coherence $\gamma(\upsilon)$ plotted as a function of the spatial frequency υ. The curve is a Gaussian curve.

5. Beam Size controlled by RF kicker

The beam sizes are also measured for the larger beam controlled by RF kicker at the region of the power (P_k) from 4mW to 500mW, and the lifetimes were measured at the same time. Figure 4 shows the spatial coherence $\gamma(\upsilon)$ of the large beam controlled in vertical direction for the various power of RF kicker. Absolute value of spatial coherence at P_k=240mW and 90mW become zero at the frequency υ=30mm^{-1} and 59mm^{-1}, respectively. These distributions suggest that the beam profiles are trapezoid. Assuming the central symmetry for the beam profile, the profile is given as a Fourier transform of the spatial coherence. The beam profile obtained by using the formula(1) at P_k=240mW is shown in fig. 5. For comparison, Fig. 5 also shows the beam profile measured by the focusing-lens imaging method at P_k=240mW.

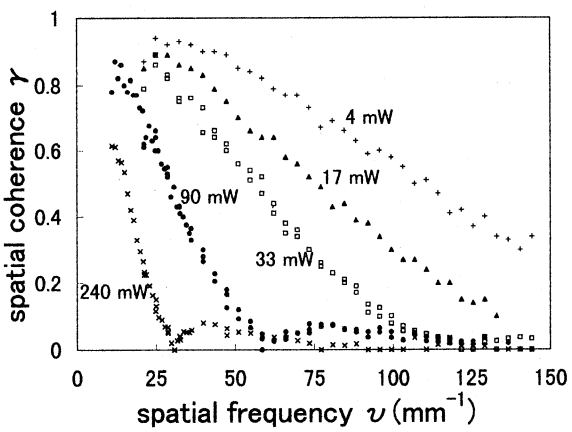

Fig. 4 Spatial coherence $\gamma(\upsilon)$ plotted as a function of the spatial frequency υ for the various beam size. Plusses, full triangles, open squares, full circles and crosses denote for 4mW, 17mW, 33mW, 90mW and 240mW of the power of RF kicker, respectively.

The solid curve (SR interferometer) and the dashed curve (focusing-lens imaging method) in fig. 5 show trapezoidal distributions. We can consider the trapezoidal beam profile is due to a sinusoidal potential of RF kicker.

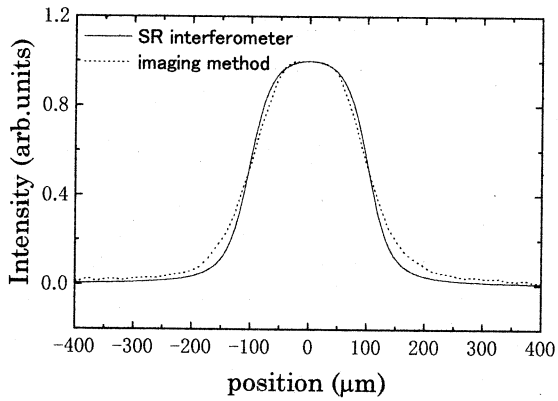

Fig. 5 Beam profiles at P_k=240mW. Solid and dashed curves correspond to the curve obtained by using the SR interferometer and the focusing-lens imaging method, respectively.

6. Beam Size and Lifetime

Figure 6 shows the measured lifetimes and the Touschek lifetime[4,5] as a function of the beam size. The Touschek lifetime is given by

$$\tau_t = \frac{\gamma_E^2 \eta^2}{4\pi r_0^2 c} \frac{v_b}{N_b} \frac{1}{J(\eta, \delta q)} \qquad (4)$$

where, v_b is the bunch volume, N_b the number of electrons per bunch, δq rms transverse momentum in unit of m_0c, η the maximum relative energy deviation accepted by the RF system, γ_E the stored electron energy in unit of m_0c^2, r_0 the classical electron radius. The function J is given by

$$J = \frac{(1+\delta p^2)^{1/2}}{\delta p} + \frac{1}{2\delta p}\left\{\ln\left(\frac{2}{\eta}\right) - \frac{23}{4} + \frac{1}{2}\ln\left[\frac{(1+\delta p^2)^{1/2}-1}{(1+\delta p^2)^{1/2}+1}\right] + \frac{2}{\delta p}\ln\left(\delta p + (1+\delta p^2)^{1/2}\right)\right\} \qquad (5)$$

In the case of the small beam size, the measured lifetime agree with the Touschek lifetime, otherwise the lifetime obtained for the large beam size deviate the Touschek lifetime. This result suggest that the Touschek effect is dominant factor and gas scattering affect the lifetime for the large beam size.

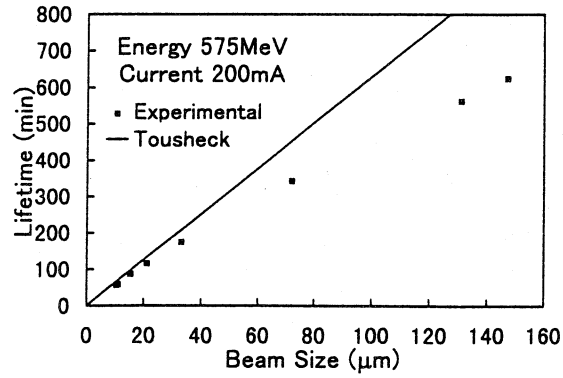

Fig. 6 The lifetime as a function of the vertical beam size.

Acknowledgments

Authors with to thank to Mr. T. Nakayama and Mr. M. Yamamoto for their aid in the recording of the interferogram.

Reference

[1] M. Born and E. Wolf, "Principles of Optics", Pergamon press. (1980)

[2] T. Mitsuhashi, N. Hiramatsu, N. Takeuchi, M. Itoh and T. Yatagai, Proc. 11th Symp. on Accelerator Science and Technology, Harima, pp273 (1997)

[3] D. Amano, T. Hori, H. Iwasaki and Y. Yamamoto, Abstract of Inter. Workshop Study the Future Functions of Small Storage Rings and Free Electron Lasers, Okazaki, p11 (1997)

[4] C. Bernardini, G. F. Corazza, G. Di Giugno, G. Ghigo, J. Haissinski, P. Marin, R. Querzoli and B. Touschek, Phys. Rev. Lett., **10** (1963) 407

[5] R. P. Walker, Proc. of IEEE Particle Accelerator Conference, p.491(1987)